Student Name: Adam Yan

Date: August 8th 2014

Project Title: Molecular Characterization of Circulating Tumor Cells Isolated from the Peripheral Blood of Prostate Cancer Patients

Primary Supervisor Name: Dr. Sabine Mai

Department: Manitoba Institute of Cell Biology, University of Manitoba, CancerCare Manitoba, Winnipeg, Manitoba, Canada.

Summary: Due to the high prevalence and morbidity associated with prostate cancer, and the absence of a reliable and effective screening tool, we have sought to evaluate the potential role of telomere profiles and circulating tumor cells (CTCs) in filling this void. CTCs can be isolated from the blood of patients and used to profile the molecular characteristics of the primary tumor they derive from. Utilizing a quantitative fluorescence in-situ hybridization (Q-FISH) protocol and our Teloview™ program, we can analyze the telomeres contained within these cells. It has been proven that increasing telomere dysfunction can be correlated with increasing aggressiveness in various cancers. In this study we were able to successfully isolate CTCs from all prostate cancer patients enrolled in our study irrespective of disease stage. We were also able to produce a unique telomere profile for each patient. When repeat analysis of telomere profiles was done, we demonstrated that some patients had stable profiles, some had minor changes, and some had substantial changes. We have linked these changes to the clinical interventions used to manage the patient's disease. Using a statistical analysis system we categorized individual telomeres as low, medium or high intensity, and measured the peak telomere number (PTN) for each patient. Combining this information has allowed us to create a model to stratify patients based on their risk of disease progression. In the future this system may replace conventional screening, and prognostication methods, and aid in the development of a more personalized approach to treating prostate cancer.

[redacted]

Acknowledgments: I gratefully acknowledge the support by one or more of the following sponsors; CancerCare Manitoba, H.T. Thorlakson Foundation, Manitoba Medical Services Foundation, Dean, Faculty of Medicine, Associate Dean (Research) Faculty of Medicine, Manitoba Health Research Council, Manitoba Institute of Child Health, Kidney Foundation of Manitoba, Leukemia and Lymphoma Society of Canada, Heart and Stroke Foundation, Health Sciences Center Research Foundation, The June Helen Coulter Memorial BSc(Med) Scholarship, Ride for DAD, Movember, GAP1 Manitoba, MITACS Accelerate and Carl Zeiss Canada.

Introduction

With an estimated 240,890 newly diagnosed cases of prostate cancer in the United States each year, prostate cancer poses a significant threat to men's health [1]. In 2014 the Canadian Cancer Society predicts that prostate cancer will be the most frequently diagnosed cancer, and the third most common cause of cancer related death for Canadian men [2,3]. Prostate cancer is a slowly progressing disease and thus offers medical personnel ample time to intervene with potentially life-saving therapies. Establishing a reliable screening and monitoring tool for prostate cancer is a crucial step in ensuring the timely and accurate identification of the disease.

One test that has been widely studied and utilized for screening and monitoring purposes measures the serum levels of prostate specific antigen (PSA). PSA is a glycoprotein secreted from the epithelial cells of the prostate. PSA levels can be elevated in prostate cancer and other prostate-related conditions such as benign prostate hyperplasia (BPH) and prostatitis [4-6]. Since PSA is a non-specific marker, an elevated serum level may cause physicians to mistake a benign prostatic condition for a more ominous prostate cancer. Studies looking at the efficacy of PSA screening have revealed that there are similar rates of prostate cancer diagnosis between screened and unscreened populations [7]. One study found that of the 1014 men they diagnosed with prostate cancer, 293 of those patients would not have had a decrease in their quality of life had the tumor not been identified [8,9].

It is clear that there are severe limitations to the current PSA screening test being conducted around the world. Other biomarkers for prostate cancer include assessing gene rearrangements involving TMPRSS22-ERG or ETS, amplifying and measuring the androgen receptor (AR), and looking for PTEN loss [10]. Even in combination none of these extensively studied biomarkers are able to reliably predict disease behavior. The Gleason Grading system evaluates prostate pathology obtained via biopsy and assigns two numbers between 1-5 based on the microscopic appearance of the cells. The first number reported is often called the primary grade and represents the most common pathology seen. The second number reported is often called the secondary grade and represents the second most common pathology seen. The two numbers are then summed together to yield the final Gleason score, which can range from 2-10. Higher numbers represent increasingly aggressive variants of prostate cancer. For instance a patient with a 4+3=7 Gleason score has a worse prognosis than a patient with a Gleason score of 3+4=7. The Gleason Grading system is effective at stratifying patients, however the requirement of biopsy specimens renders gross pathological monitoring with substantial limitations.

The absence of a suitable mechanism of monitoring prostate cancer gives rise to the demand to develop an alternative tool. One postulated method of screening for prostate cancer and following the course of established disease is to analyze the patient's circulating tumor cells (CTCs). CTCs originate from primary tumors and are shed into the patient's circulation [11]. Since CTCs are histologically similar to the tumor they derive from, they can be used for biological tests that seek to investigate properties of the original tumor [11].

In order to utilize CTCs as a screening tool, an efficient and reliable method of CTC isolation must be developed. Numerous CTC isolation methods have been explored, however severe limitations render most of these methods unsuitable for this study. It is important to develop an extremely sensitive isolation method due to the rarity of CTCs described, 1 per 10^9 cells in peripheral blood [11]. A common method of isolation is based on the selection of cells with specific surface antigens. Commonly a magnetic bead-conjugated antibody against epithelial-cell adhesion molecule (EpCAM) is used to identify CTCs. This method is based on the

assumption that the presence of epithelial markers in the blood stream is indicative of cancer. However, numerous healthy controls were found to have epithelial cells in their circulation [11]. Furthermore, the EpCAM based filtration method fails to detect tumors that are non-epithelial in origin such as melanoma, "normal" type breast cancers, and cells that have lost their epithelial antigens after having undergone the epithelial to mesenchymal transition (EMT) [11]. EpCAM filtration methods could not be utilized for our study since many prostate cancer CTCs do not express EpCAM. A second method is to use reverse transcription-polymerase chain reaction (PCR) based assays. Unfortunately, the RNA extraction process used in this method destroys the cell integrity and is limited overall due to its ineffectiveness at distinguishing CTCs from circulating non-tumor cells [12]. Gradient centrifugation is able to separate mononucleated cells from red blood cells (RBCs) based on their differing buoyant densities through a Ficoll-Hypaque separation protocol [13]. This approach is limited due to the minimal contribution of CTCs to the total mononucleocyte population and a failure of the methodology to capture the majority of the CTCs present [13]. A final mechanism often employed is the nucleic acid-based detection of CTCs using free DNA, RNA, and/or miRNA circulating in the patient's plasma. This protocol cannot ensure that the origin of the nucleic acid is CTC in origin and not from necrotic cells in the tumor deposits, tumor-derived exosomes, or cellular fragments [13]. The free nucleic acids used are liberated from dead CTCs. It is currently unclear if the information gained from analyzing dead CTCs is relevant since the information does not relate to the living CTCs present. The protocol also has a low sensitivity, and the interpretation of a negative test is difficult due to the inability to distinguish insufficient amounts of tumor-derived DNA from the true absence of tumor-derived DNA [13]. Our study was able to overcome the limitations of the five previously described methodologies through the use of a ScreenCell size-based isolation protocol. The ScreenCell device has circular pores (diameter of 7.5 ± 0.36 μm) that prevent the movement of prostate cancer cells (typical diameter of15-25 μm) through the filter.

Telomeres are the ends of eukaryotic chromosomes. Upon isolation of the CTCs, analysis of the telomeres can be used to profile the CTCs of prostate cancer patients. It has been shown that many cancer patients experience chromosomal instability (CIN) due to telomere dysfunction [9]. Somatic cells generally lack telomerase, the enzyme that replenishes the telomeres, and thus the continuous proliferation of tumor cells results in a shortening telomere [14]. Without the telomeres capping and protecting the chromosome ends, the cell recognizes their structure as DNA breaks, and chromosomes may be joined by their ends causing the initiation of the break-fusion bridge cycle and CIN [14]. It has been proven that head, neck, lung, renal cell, and bladder cancer patients have telomeres that are significantly shorter than a healthy control's telomeres [15]. Telomeres are normally arranged in a contrived non-overlapping manner in the cells nucleus [12]. Cancer cells frequently exhibit pathological variations of the normal telomeric organization and can be found as telomeric aggregates (TAs) [12]. It has been shown that many of the cancer cells implicated in prostate cancer are the result of telomere dysfunction [16,17]. An advancement of tumor progression and the relative aggressiveness of the tumor can be correlated to the degree of CIN seen within a given cell [18].

This study seeks to determine how the CTC profiles of prostate cancer patients match with clinical outcomes in hopes of developing surrogate biomarkers of disease using CTCs and their molecular features. This study has been able to show for the first time that patients with prostate cancer have unique telomeric profiles that correlate with their prostate cancer stage. This is of paramount significance since CTCs have been shown to have the potential to enhance cancer staging and prognostication [10-12, 19].

Materials and Methods

Patients

This research was approved by the Research Ethics Board on Human Studies at the University of Manitoba with the Ethics Reference Number: HS14085(H2011:336). The Prostate Centre at CancerCare Manitoba provided samples obtained from consenting patients. Approximately 8 ml of blood was obtained via phlebotomy at each visit. To ensure an unbiased sample analysis, clinical data was requested only once all laboratory tests were completed. Using the clinical data patients were stratified into four groups based on their risk of disease progression as determined by their PSA value and Gleason score. Low-risk patients were those with a Gleason score of $\leq$6, intermediate favorable-risk patients were those with a Gleason score of 3+4=7 and a stable PSA $\leq$20, intermediate unfavorable-risk patients were those with a Gleason score of 4+3=7 and an unstable PSA >20, and high-risk patients were those with a Gleason score $\geq$8 or demonstrated metastatic disease.

CTC Isolation by ScreenCell Filtration

The ScreenCell filtration device utilizes a microporous membrane filter to isolate CTCs based on size. These devices are able to isolate the complete CTC population from a given sample, as opposed to other isolation mechanisms, which often only isolate subsets of the total CTC population [7]. 3 ml of the blood sample is diluted with 4 ml of FC2 buffer. After standing for 8 minutes the diluted sample is passed into the filtration tank. Cells collect on the filter membrane due to the suction provided by the EDTA tube contained within the nozzle below the filter. The filter membrane has circular pores (diameter of 7.5 ± 0.36 μm) that prevent the movement of prostate cancer cells (typical diameter of 15-25 μm) through the filter [7,8]. The device has been validated using H2030 tumor cells. When 2 or 5 tumor cells were spiked in 1 ml of blood the ScreenCell filtration devices were able to recover 1.48 (SD, 0.71) and 4.56 (SD, 0.71) cells respectively. This resulted in an overall recovery rate of 91.2% [7].

Three-dimensional Quantitate Fluorescence in Situ Hybridization (Q-FISH)

The nuclei of the captured CTCs were subjected to Q-FISH. Filters were incubated in 3.7% formaldehyde/1xPBS, 50 μg/ml pepsin in 0.01 N HCl, and then post-fixed to the filters using 3.7% formaldehyde/1xPBS spending 10 minutes in each solution. The cells were then dehydrated using increasing concentrations of ethanol (70%, 90%, & 100%). Next 6 μl of Cyanine 3 (Cy3)–labeled peptide nucleic acid probe specific for the telomeres purchased from DAKO (Glostrup, Denmark) was applied. A coverslip and rubber cement was used to seal the filter onto the slide and prevent the Cy3 probe from evaporating. The sealed slides were placed in a Hybrite (Vysis/Abbott) thermocycler for a 3 minute denaturation at 80°C, followed by a 2 hour hybridization at 30°C. The filters were then subjected to two 15 minute washes in 70% formamide/10 mM Tris (pH 7.4), a 5 minute wash in 0.1× SSC at 55°C, and then two washes in 2× SSC/0.05% Tween 20 for 5 minutes each. In order to identify the margins of the cell's nuclei they were stained with 50 μl of 0.1 μg/ml 4′,6-diamindino-2 phenylindole (DAPI). Finally the cells were dehydrated using increasing concentrations of ethanol (70%, 90% and 100%), mounted, and cover-slipped using Vectashield reagent (Vector Laboratories, Burlington, Ontario) in order to ready the filters for imaging.

Immunohistochemistry

Some of the filter bound CTCs were subjected to immunohistochemistry as well. This was done in order to confirm that the isolated cells were in fact CTCs. Cells were fixed using 3.7% formaldehyde/1xPBS for ten minutes and then washed in two subsequent batches of 50 mM $MgCl_2$ for 5 minutes each. Filters were blocked with serum for 30 minutes. Primary filters received 50 μl of Cytokeratin 8, 18, 19, (ab41825, ABCAM^R) and 50 μl of CD45 antibodies (ab10558, ABCAM^R) both at 1 μg/μl, while control filters received 100 μl of serum. Both primary

and control filters were incubated for 30 minutes at 37°C. Filters were then washed again using PBS and 50mM $MgCl_2$ and blocked with 50 µl of serum for 30 minutes at 37°C. A mixture of 50 µl of Sheep anti-rabbit Cy3 antibody (2° antibody for CD45) and 50 µl of Goat anti-mouse IgG Alexa 488 (2° antibody for Cytokeratin 8, 18, 19) both at 1 µg/µl was incubated with the filters at 37°C for 45 minutes. Then filters were washed in PBS and 50 mM $MgCl_2$ and stained with 50 µl DAPI (1µg/µl). Finally cells were dehydrated using increasing concentrations of ethanol (70%, 90%, and 100%), and cover-slipped using Vectashield.

Three-Dimensional Image Acquisition

A Carl Zeiss AxioImager Z2 microscope (Carl Zeiss, Toronto Ontario) equipped with an AxioCam HR B&W camera and 63×/1.4 oil objective was used to acquire the necessary images. In order to image the cells that had undergone Q-FISH the Cy3 and DAPI filters on the microscope were used for the detection of peptide nucleic acid-probe hybridized telomeres and detection of nuclear DNA respectively. Using the Axiovision 4.8 software (Carl Zeiss), 80 stacks of images were taken at x=102 nm, y=102 nm, and z=100 nm with the DAPI filter, and then with the Cy3 filter. The acquisition time was 546 ms. For immunostaining studies the same software and imaging parameters were utilized, however images were taken with the microscope's Cy3, DAPI, and cytokeratin filters. From these images CTCs were identified based on their morphology and "cut" out from the surrounding image using the Axiovision 4.8 software. The images were then deconvoluted and exported as .tiff files also using Axiovision 4.8.

TeloVew™ Enabled Three-Dimensional Image Analysis and Statistical Considerations

TeloView ***™*** software is a set of DIPimage tools created for the MatLab program by our lab group [12]. Teloview ***™*** is a semi-automated program that is able to localize probes hybridized to the telomeres and integrate the intensity of the probe [12]. Teloview ***™*** can quantify various parameters such as telomere number, signal intensity, size, and distribution, as well as the number of tumor aggregates (TAs) present, and the cell's nuclear volume [8]. A TeloView***™*** analysis was done for 30 cells in each sample, and two-dimensional (2D) as well as three-dimensional (3D) images of the cells were acquired. The software was then able to synthesize graphs for each sample showing telomere number on the y-axis and signal intensity on the x-axis. For every sample analyzed, telomeres with intensities less than 6,000 a.u. were classified as low intensity, those with intensities between 6,000-20,000 a.u. were classified as intermediate intensity, and those with intensities above 20,000 a.u. were classified as high intensity. The percentage of telomere signals in the low, intermediate, and high signal intensity groups was determined using a Statistical Analysis System (SAS).

TeloScan Enabled Three-Dimensional Image Analysis

As a more clinically applicable alternative to the 3D image acquisition and Teloview ***™*** enabled 3D image analysis steps, analysis was performed using TeloScan. TeloScan is an automated 3D scanning system being developed by the Mai Lab in conjunction with Applied Spectral Imaging (ASI). TeloScan can be paired with the same microscope and imaging protocol described previously [14]. Instead of selecting a subset of the cells present and using them as a representation of the entire CTC population, TeloScan is able to scan the entire filter using the Genasis software (Applied Spectral Imaging) to enumerate the CTCs present. Like TeloView ***™*** it is able to quantify the telomere number, telomere intensities, and the number of TAs present [14]. In a study of glioblastoma tumor cells it was found that TeloView ***™*** and TeloScan led to identical categorization of patients [14]. TeloScan has a rapid processing speed and the ability to analyze a large number of cells. These advantages make TeloScan a more appropriate candidate for future widespread clinical use.

Results

Confirmation of CTC Identification

The cells identified morphologically were immunostained to confirm that they were indeed CTCs. The ScreenCell filtration device captures all cells larger than its pores, so it is necessary to ensure that incidentally captured lymphocytes were correctly omitted during analysis. During immunostaining an antibody that localizes to unique cytokeratins (8, 18, and 19) found on CTCs can definitively differentiate CTCs from lymphocytes. Cells appearing with a green ring surrounding them are CTCs, while those without the distinctive ring are not. The cells identified by immunostaining were cytokeratin positive as demonstrated by the presence of a green ring surrounding the cell (Figure 1). This indicates that we were in fact isolating and analyzing CTCs in subsequent experiments. Work is underway to perform an additional immunohistochemistry experiment whereby an anti-androgen receptor antibody is used. The presence or absence of this receptor on the isolated CTCs will allow us to determine if the isolated CTCs retain this characteristic feature of the primary prostate tumor.

CTCs Identified in All Stages of Prostate Cancer

Utilizing the ScreenCell size-based filtration system CTCs have been recovered from the blood of all 250+ patient samples analyzed to date. CTCs were readily isolated from patients within the metastatic, high-risk, intermediate-risk, as well as low-risk patient groups. At minimum 30 CTCs are needed to carry out TeloView ***TM*** analysis on these patient samples. Most of the patients in this study have had more than 30 CTCs identified in the 3 mls of blood used, while a smaller subset had less than 30 cells identified. This disproves the belief that the presence of tumor cells circulating in a patient's blood is pathognomonic of metastatic disease. A more in depth analysis of the molecular structure of the CTCs reveals that the CTCs isolated in each stage of disease are unique. The correlation of various disease states to CTC nomenclature gives rise to the utility of CTCs in molecular diagnostics and patient monitoring. Determining the relative concentration of CTCs per milliliter of blood may offer an additional perspective on disease evolution, however the absolute CTC number may not necessarily reflect the aggressiveness of the cancer.

Automated Scanning and Enumeration of CTCs Using TeloScan

Using software custom designed by our lab in conjunction with Applied Spectral Imaging (ASI) automated CTC enumeration was undertaken using two different methods. The first is a size-based approach that identifies DAPI stained nuclei. The second is a cytokeratin-based approach, which detects cells stained with an antibody that localizes only to unique cytokeratins (8, 18 & 19) on CTCs. The preliminary CTC enumeration results are presented in Table 1. The TeloScan results do confirm our initial conclusion from TeloView that CTCs are present in all stages of disease. Moreover, it does appear that the DAPI size-based and cytokeratin-based methods yield similar enumeration results. The mean percent difference between the two enumeration methods was 9%. No obvious correlation between stage and CTC number is apparent at this time, however too few samples have been analyzed to make any meaningful conclusions.

Telomeres of CTCs Shorten and/or form Aggregates as Cancer Advances

In human cells the length of the telomere decreases by 50-200 bases with each cell division [20]. Due to their rapid proliferation, cancer cells are plagued by two forms of telomeric dysfunction. The first is the formation of critically short telomeres, and the second is the formation of telomeric aggregates [21-23]. It has been shown that telomeric aggregates are formed independently of telomere size or telomerase activity [21,23]. The management of prostate cancer can be improved through the development of an algorithm that utilizes the telomeric signatures of prostate CTCs. With progression of the tumor the telomeres shorten.

Telomeres may shorten to a critical length where the optical resolution of the microscope (x=102 nm, y=102 nm, and z=200 nm) precludes our ability to detect these telomeres. This may cause a lower than expected number of telomeres to be seen in advanced cancer cells when a plot of telomere number (y-axis) vs. telomere intensity (x-axis) is obtained from TeloView*TM* [23]. The clinical data of selected representative patient's is presented in Table 2 along with the corresponding Teloview*TM* data. Subpopulations of telomeres with differing intensities can be visualized within a given telomere population. The percent of telomeres in each of these subpopulations is calculated for each patient. A correlation of the clinical and telomeric parameters allows for an appreciation of the genomic stability observed within the context of the patient's clinical progression. Our work proposes that through the analyses of telomeric profiles, eminent shifts in clinical profiles may be detected earlier by telomeric analysis than by current means.

Unique 3D Telomere Profiles of CTCs Identified

In previous work published by our lab group in 2013, we were able to demonstrate that different tumor types such as prostate, colon, breast, melanoma, and lung have unique CTC subpopulations [11]. In this study, analyses of the telomeres at different stages of prostate cancer allowed for a greater understanding of the changes in telomere profiles that occurs with disease evolution. For this study patients were stratified into four groups based on their risk of disease progression as determined by their PSA value and Gleason score.

Plots of telomere number vs. telomere intensity are obtained from Teloview*TM*. Figure 2 demonstrates the 3D nuclear telomeric profiles of patients with varying risks of disease progression. Figure 2A shows the profile of patient MB0221 in June 2012. This patient has a low risk of disease advancement based on his clinical profile of Gleason 3+3=6 and PSA of 5.13. The graph shows a wide distribution of telomere intensities and an intermediate peak telomere number (PTN). The PTN is the number of telomeres present at the most commonly occurring telomere intensity. The PTN can be visualized on the Teloview*TM* graphs as the highest point on the y-axis. These properties are characteristic of the graphs obtained from low-risk patients.

Figure 2B shows the profile of patient MB0261 in April 2013. This patient has a high-risk of progression due to his Gleason score of 4+5=9. This patient has no evidence of metastatic disease. This patient's graph demonstrates a high number of short telomeres seen as a "cliff" peak in Teloview*TM*. These properties are characteristic of the graphs obtained from high-risk patients.

Figure 2C and 2D are derived from the intermediate-risk Gleason 7 patients MB0235 in August 2012 and MB0241 in August 2012 respectively. The intermediate-risk group is divided into the favorable-risk cohort with Gleason 3+4=7 and PSA $\leq$20, and the unfavorable cohort with Gleason 4+3=7 and PSA >20. Intermediate-risk patients demonstrate a variety of patterns in their telomere signal plots. These patients often have two or three subpopulations of telomeres and wide variations in the number and size of the telomeres present. This can be attributed to the varying levels of aneuploidy of patients in this broadly grouped category. Figure 2C shows patient MB0235 who is a favorable intermediate-risk patient with Gleason 3+4=7 and three sub-populations of telomeres. Figure 2D shows patient MB0241 who is an unfavorable intermediate-risk patient with Gleason 4+3=7 and three subpopulations of telomeres.

Shifts in Telomeric Signatures May Reflect Early Shifts in Prostate Cancer Stages for Intermediate-Risk Patients

Analysis of multiple samples from the same patient over a period of 6-months to 1-year gives rise to the ability to monitor changes in the patient's telomeric signature. Using three

favorable intermediate-risk patients all enrolled in an active surveillance program we can appreciate the varied progression of a telomere profile when medical intervention is withheld. As demonstrated in Figure 3 patients were found to either have a stable profile (Fig.3A), an intermediate change in their profile (Fig.3B), or a significant change in their profile (Fig.3C). The green curve represents the first sample examined and the red curve depicts the repeat sample examined at a later time point. The stable telomeric profile depicted in Fig.3A was derived from the patient MB0256 over the period of November 2012 to March 2013. The stability of the telomere profiles indicates a stable aneuploidy state and suggests a low aggressiveness of the cancer. Figure 3B and 3C were obtained from the patients MB0241 and MB0266 respectively and illustrate the ongoing genomic changes occurring in these patients. The changes in Fig.3C are more profound than those in Fig.3B indicating a more rapid progression of telomeric change. When considered in conjunction with other clinical information, an advancing telomere profile may warrant earlier physician intervention as it reflects progressive genomic dysfunction. Patients on surveillance in the low-risk and high-risk groups have also been shown to demonstrate no change, an intermediate change, or a significant change in their telomere profiles (Table 2). Analysis of telomere profile changes can therefore be applied to patients with any degree of disease burden in order to monitor potential progression and influence clinical decision-making.

Repeat analysis of samples can also be used to show the affect of both surgical and medical management of prostate cancer on telomere evolution. As a general trend the peak telomere number (PTN) increases in the interval immediately following any medical or surgical intervention. One postulated reason for this observation is that any intervention that disrupts the prostate architecture will liberate large numbers of CTCs and these CTCs will continue to evolve in the blood stream, and seed other locations. Not all patients demonstrated an increase in PTN following treatment. Some patients had a stable PTN and some had a decrease in PTN.

Figure 4 shows the affect of both medical therapy and surgery on telomere profiles. The green curve represents the first time point sampled, the purple curve represents the second time point sampled, and the red curve represents the third time point sampled. Patient MB0211 underwent a radical prostatectomy with bilateral lymphadenectomy in May 2012. Between May 2012 and September 2012 the PTN increases significantly from 27 to 288. Repeat analysis of the patient in January 2013 shows that the PTN has dropped to 57. During the surveillance period between May and January 2013 the PTN has begun to decrease and is approaching the normal PTN of 40-60 [24]. This patient has an initial increase in his PTN following surgery, and then his PTN approaches the normal value during the follow-up period (Fig.4A).

A similar trend can be observed for patients undergoing medical management of their disease. Patient MB0212 was treated with Bicalutamide 50 mg between May and July of 2012, as well as Goserelin 10.8 mg between June 2012 and July 2013. Between May and December of 2012 the PTN increased significantly from 22 to 85. Between December 2012 and June 2013 the PTN decreases from 85 to 46. This patient has an initial increase in his PTN following the initiation of treatment, and then as the therapy is able to successfully decrease tumor burden the PTN decreases (Fig 4B). Similar results have been demonstrated with other forms of medical management including various combinations of Bicaludamide, Zoladex, Goserelin, Leuprolide, Radiation Therapy (RT), and Cryotherapy.

Proposed Telomere Profile Model for Monitoring Prostate Cancer Evolution

The molecular evolution of prostate cancer is highly variable. Both the predominant histology of the tumor and the course of treatment chosen by the patient can alter the tumor's course. It is possible to monitor the changes in the molecular profile of prostate cancer patients

through the use of 3D-imaging and telomere quantification. Utilizing established dogma on telomere evolution and relevant statistical considerations a proposed model for monitoring prostate cancer evolution has been derived. The model takes into account peak telomere number (PTN), and the telomere intensity distribution present. Low-risk patients typically demonstrate a wider distribution of telomeres with multiple subpopulations, and a PTN between 35-65. High-risk patients tend to show a more narrow distribution of telomeres with a telomere population dominated by short telomeres as demonstrated by a "cliff" peak on their Teloview^{TM} graphs. High-risk patients also tend to have a higher PTN, most commonly >65. Advanced and metastatic patients have a lower PTN, usually <35, due to the shortening of telomeres beyond the optical detection capacity of the microscope currently used to complete the analysis.

Discussion

In 2012 the United States preventative Services Task Force recommended against routine screening for prostate cancer in men of any age due to the gross overtreatment of the disease [29]. The task force noted that 30-40% of men who have undergone treatment for prostate cancer had tumors that would have never had an affect on the patient's quality of life due to the tumor's indolent nature [29]. What is alarming about this recommendation is that in the United States there has been a 45% decline in mortality rates for prostate cancer since screening programs were initiated [29]. In order to reconcile the need to identify and monitor prostate cancer to prevent deaths from the disease, and the need to limit over-diagnosis and overtreatment of prostate cancer to prevent unnecessary treatment and lower healthcare expenses, an alternative diagnostic and monitoring modality needs to be developed.

Prostate cancer lends itself nicely to studies of molecular biology. It progresses slowly which allows for subtle cellular changes to be monitored over time [29]. Prostate cancer's high prevalence and incidence rate allows for the feasible collection of the necessary number of samples needed to make meaningful conclusions [2,3]. As we foray into the era of personalized medicine understanding genomic changes in cancer brings us one step closer to providing exceptionally individualized care.

Irrespective of the patient's stage of disease, this study has been able to successfully isolate CTCs from all samples collected. In contrast, a recently published study of high-risk non-metastatic patients found that only 5 out of 36 patients analyzed had CTCs [25]. This study was also only able to isolate at maximum 3 CTCs from a 7.5 ml sample of blood [25]. We believe this stark contrast between their results and ours can be attributed to the superiority of the ScreenCell sized-based filtration protocol utilized in this experiment over their EPCAM-antibody-based CellSearch protocol. This is a reasonable conclusion to draw as the EPCAM based filtration mechanism has been proven to fail in isolating CTCs that have undergone the EMT and in isolating the large number of prostate derived CTCs that do not display EPCAM [11].

It has been shown that CTC enumeration done days apart can yield contradictory information due to the instability and fragility of the cells [26]. Since only a small amount of blood is used, the analyzed sample may not be representative of the true CTC population present. It is possible that the variations in CTC numbers are due to these limitations in CTC enumeration, and not clinically significant. However, it has been demonstrated that CTC enumeration done before and after therapy in patients with metastatic castration-resistant prostate cancer (mCRPC) could be correlated with the patient's prognosis [27,28]. Further sample analysis will allow us to make more meaningful conclusions as to the potential role of CTC enumeration in monitoring disease evolution.

Unique telomere profiles have been constructed for each sample based on the quantitative analysis of their 3D telomere structure. Through the novel coupling of the ScreenCell CTC filtration device with 3D quantitative fluorescence in situ hybridization analysis using the Teloview^{TM} program, we have shown for the first time that CTC profiles may be suitable for screening for prostate cancer and/or monitoring prostate cancer progression.

Our lab was able to demonstrate unique and distinctively tumor specific aberrations in the nuclear architecture of telomeres in colon, breast, melanoma, lung, and prostate cancer in 2013 [11]. This large cohort of prostate cancer patients allowed us for the first time to identify stage-specific profiles, and monitor the affects of various clinical interventions of telomere evolution. Other members of our lab group have already used 3D telomere architecture to help assess and profile other cancer types such as myelodysplastic syndrome, and acute myeloid leukemia into subgroups [30]. In this study we have been able to expand the use of such profiling systems to prostate cancer for the first time, and provide further validation to telomere based profiling. An understanding of advances in cancer evolution and progression through the use of telomere profiling may eventually lead to improvements in cancer management.

Monitoring the evolution of CTCs derived from prostate cancer patients is paramount in the quest to understand the behavior of prostate cancer. Identifying rapidly evolving, and aggressive cancer phenotypes will allow for more accurate prognostication, which in turn will provide more clarity as to the appropriate course of treatment for the patient. The most important application of this is in monitoring intermediate-risk patients. It is often unclear with this patient group if treatment needs to be initiated or if active surveillance is warranted. Applying 3D telomere monitoring to this patient cohort may allow us to predict those at increased risk of progression. Full exome sequencing of CTCs will allow for the correlation of 3D telomeric signatures with genetic profiles. Ultimately when considered in tandem with CTC enumeration results, these molecular characteristics can be correlated to chance of disease progression in order to produce evidence-based guidelines for disease monitoring and management. There is potential that certain CTC subpopulations(s) may be more effectively targeted by different therapies, and this knowledge may alter treatment plans. This opens up a new niche of pharmacologic innovation whereby drugs can be developed that target-specific CTC subpopulation(s). For instance, it has already been demonstrated that not all CTC possess the malignant traits necessary to cause disease metastasis [31]. Therefore it may be possible to develop treatments that specifically target this subset of CTCs that are responsible for metastasis.

We have proposed and described an initial model for stratifying prostate cancer patients based on the evolution of their telomere profile. To date we have analyzed 250 samples from 73 different patients. The proposed model needs to be further validated using a larger patient population with an extended follow up period. The remaining 500 unanalyzed samples that we have filtered should provide an excellent strength to this project. Further work also needs to be done to automate the TeloScan software to reliably and consistently identify and analyze prostate cancer CTCs correctly. The automated nature of this program makes it a feasible and economically viable option for future widespread clinical implementation. Once the proposed telomere profiling model has been validated, and the TeloScan software fully automated, the two can be coupled for clinical identification, stratification, and monitoring purposes.

References

[1] Gomella LG, Liu XS, Trabulsi EJ, et al. Screening for prostate cancer: the current evidence and guidelines controversy. J Urology. 2011:18(5)5875–5883.
[2] Crawford ED. Epidemiology of prostate cancer. J Urology. 2003:22(62)3-12.
[3] Canadian Cancer Society's Advisory Committee on Cancer Statistics. Canadian Cancer Statistics 2014.Toronto, ON: Canadian Cancer Society; 2014.
[4] Venderbos LDF, Roobol MJ. PSA-based prostate cancer screening: the role of active surveillance and informed and shared decision making. Asian J Androl. 2011;13(2):219–24.
[5] Chou, R, Croswell, JM, Dana, T, et al. Screening for Prostate Cancer: A Review of Evidence for the U.S. Preventive Services Task Force. Ann of Inter Med. 2011;155(11):762–784.
[6] Scher HI, Morris MJ, Kelly WK, Schwartz LH, Heller G. Prostate cancer clinical trial end points: "RECIST"ing a step backwards. Clinical cancer research : an official journal of the American Association for Cancer Research. 2005;11(14):5223-32.
[7] Lin, K, Lipsitz R, Miller T, Janakiraman S. Benefits and Harms of Prostate-Specific Antigen Screening for Prostate Cancer: An Evidence Update for the U.S. Preventive Services Task Force. Ann Internal Med; 149(3):192–199.
[8] Schröder FH. Screening for prostate cancer (PC)--an update on recent findings of the European Randomized Study of Screening for Prostate Cancer (ERSPC). Urologic oncology. 2008;26(5):533–41.
[9] Schröder FH, Bangma CH, Roobol MJ. Is it necessary to detect all prostate cancers in men with serum PSA levels <3.0 ng/ml? A comparison of biopsy results of PCPT and outcome-related information from ERSPC. European Urology. 2008;53(5):901–8.
[10] Eckersberger E, Finkelstein J, Sadri H, Margreiter M, Taneja SS, Lepor H, et al. Screening for Prostate Cancer: Review of the ERSPC and PLCO Trials. Reviews in urology. 2009;11(3):127-33.
[11] Desitter I, Guerrouahen BS, Benali-Furet N, Wechsler J, Jänne PA, Kuang Y, Yanagita M, Wang L, Berkowitz JA, Distel RJ, et al. A new device for rapid isolation by size and characterization of rare circulating tumor cells. Anti-cancer Res. 2011:31: 427–441.
[12] Adebayo JA, Xu M, Wechsler J, Benali-Furet N, Cayre YE, Saranchuk J, DracHenberg D, Mai M. Three-Dimensional Telomeric Analysis of Isolated Circulating Tumor cells (CTCs) Defines CTC Subpopulations. Trans Onc. 2013(6):1:51-65.
[13] Yu M, Stott S, Toner M, Meheswaran S, Haber D. Circulating tumor cells: approaches to isolation and characterization. J Cell Bio. 2011(192):3:373-382
[14] Wu X, Amos C, Zhu Y, Zhao H, Grossman BH, Shay JW, Luo S, Hong WK, Spitz MR. Telomere dysfunction: a potential cancer predisposition factor. J Natl. Cancer Inst. 2003:95(16):1211-1218.
[15] Heneriques CM, Ferreira MG. Consequences of telomere shortening during lifespan. Curr Opin Cell Biol. 2012:24(6):804-808.
[16] Selvarajah S, Yoshimoto M, Park PC, Maire G, Paderova J, Bayani J, et al. The breakage-fusion-bridge (BFB) cycle as a mechanism for generating genetic heterogeneity in osteosarcoma. Chromosoma. 2006;115(6):459-67.
[17] Vukovic B, Park PC, Al-Maghrabi J, Beheshti B, Sweet J, Evans A, et al. Evidence of multifocality of telomere erosion in high-grade prostatic intraepithelial neoplasia (HPIN) and concurrent carcinoma. Oncogene. 2003;22(13):1978-87.
[18] Mai S and Garini Y. The significance of telomeric aggregates in the interphase nuclei of tumor cells. J Cell Biochem. 2006:97:904–915.
[19] Gross HJ, Verwer B, Houck D, Hoffman RA, Recktenwald D. Model study detecting breast cancer cells in peripheral blood mononuclear cells at frequencies as low as 10(-7). Proceedings of the National Academy of Sciences of the United States of America. 1995;92(2):537-41.
[20] Lansdorp PM. Repair of telomeric DNA prior to replicative senescence. Mechanisms of ageing and development. 2000;118(1-2):23-34.

[21] Louis SF, Vermolen BJ, Garini Y, Young IT, Guffei A, Lichtensztejn Z, et al. c-Myc induces chromosomal rearrangements through telomere and chromosome remodeling in the interphase nucleus. Proceedings of the National Academy of Sciences. 2005;102(27):9613-8.
[22] DePinho RA, Polyak K. Cancer chromosomes in crisis. Nature genetics. 2004;36(9):932-4.
[23] Chuang TC, Moshir S, Garini Y, Chuang AY, Young IT, Vermolen B, et al. The 3D organization of telomeres in the nucleus of mammalian cells. BMC biology. 2004;2:12.
[24] De Vos WH, Hoebe RA, Joss GH, Haffmans W, Baatout S, Van Oostveldt P, et al. Controlled light exposure microscopy reveals dynamic telomere microterritories throughout the cell cycle. Cytometry Part A : the journal of the International Society for Analytical Cytology. 2009;75(5):428-39.
[25] Loh J, Jovanovic L, Lehman M, Capp A, Pyror D, Harris M et al. Circulating tumor cell detection in high-risk non-metastatic prostate cancer. J Cancer Res Clin Oncol. 2014
[26] Qin J, Alt JR, Hunsley BA, Williams TL, Fernando MR. Stabilization of circulating tumor cells in blood using a collection device with a preservative reagent. Cancer Cell Int. 2014;14(1):23
[27] Goldkrom A, Ely B, Quinn DI, Tangen CM, Fink Lm, Xu T, et al. Circulating tumor cell counts are prognstic of overall survival in SWOG S0421: a phase III clinical trial of docetaxel with or without atrasentan for metastatic castration-resistant prostate cancer. J Clin Oncol. 2014;32(11):1136-42
[28] Miyamoto DT, Sequist LV, Lee RJ. Circulating tumour cells-monitoring treatment response in prostate cancer. Nat Rev Clin Oncol. 2014;(7):401-12
[29] Cooperberg, M. Improving methods to identify indolent versus aggressive prostate cancer. Poster session presented at the Annual Meeting of the American Association of Cancer Researchers; 2014 April 5-9; San Diego, CA USA.
[30] Gadji M, Adebayo Awe J, Rodrigues P, Kumar R, Houston DS, Klewes L, et al. Profiling three-dimensional nuclear telomeric architecture of myelodysplastic syndromes and acute myeloid leukemia defines patient subgroups. Clinical cancer research : an official journal of the American Association for Cancer Research. 2012;18(12):3293-304.
[31] Yao X, Choudhury AD, Yamanaka YJ, Adalsteinsson VA, Gierahn TM, Williamson Ca, et al. Functional analysis of single cells identifies a rare subset of circulating tumor cells with malingnat traits. Integr Biol (Camb). 2014;(4):388-98

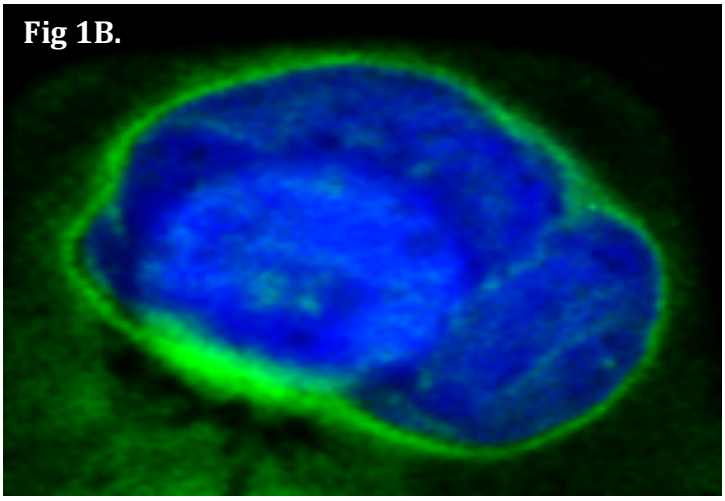

Figure 1: Confirmation of Correct CTC Identification.
Immunostaining was done to confirm that the cells used for analysis in TeloView*TM* were in fact CTCs. The cytokeratin probe localizes only to unique cytokeratins found on CTCs, and causes the cell to appear with a green border when imaged. Fig 1A shows a lymphocyte with no green stain, while Figure 1B shows a CTC with green stain localizing around its perimeter.

PATIENT ID	CLINICAL STAGE	PSA µg/L (MM/YY)	GLEASON SCORE BY TRUS (MM/YY)	CYTOKERATIN STAINED CTCs/mL	DAPI SIZE-BASED CTCs/mL	PERCENT DIFFERENCE BETWEEN CYTOKERATIN AND DAPI RESULTS:
MB0353-09-13	Favorable intermediate-Risk	<0.01 (11/13)	3+4 (11/13)	30	40	28.6
MB0339-07-13	Favorable intermediate-risk	<0.01 (10/13)	3+4 (06/13)	198	204	3.0
MB0251-05-13	Unfavorable intermediate-risk	3.03 (05/13)	4+3 (09/11)	30	32	6.5
MB0251-09-13	Unfavorable intermediate-risk	3.31 (11/13)	4+3 (09/11)	242	239	1.3
MB0171-08-13	High-risk non-metastatic	0.09 (08/13)	4+5 (01/12)	70	100	25
MB0282-04-13	High-risk metastatic	47.00 (04/13)	4+5 (12/12)	86	80	7.2
MB0301-03-13	High-risk metastatic	40.00 (03/13)	4+4 (10/12)	190	169	11.8

Table 1: Comparison of Selected CTC Enumeration Results Using Cytokeratin and DAPI-Size-Based Protocols.
CTCs were identified in all samples analyzed. The cytokeratin and DAPI size-based methodologies are able to yield similar enumeration results.

PATIENT ID	PERCENTAGE (%) OF TELOMERE INTENSITY SUBPOPULATIONS IN THE SAME PATIENT			TELOMERIC PROFILE	PSA µg/L (MM/YY)	GLEASON SCORE (GS) BY TRUS (MM/YY)	CLINICAL INTERVENTIONS	PEAK TELOMERE NUMBER	AVERAGE NUCLEAR DIAMETER (µm)
	LOW	MEDIUM	HIGH						
LOW-RISK (GS ≤6)									
MB0221-06-12	14.9	56.7	28.4	Stable	5.13 (05/12)	3+3 (05/10)	Active Surveillance	42	15.1
MB0221-12-12	24.4	58.7	16.9		7.39 (11/12)			45	10.1
MB0276-12-12	23.2	52.0	24.8	Significant Change	9.05 (10/12)	3+3 (01/13)	Radical Prostatectomy with Bilateral Pelvic Lymphadenectomy (01/13)	34	10.63
MB0276-05-13	33.1	48.2	18.7		0.09 (03/13)			65	11.9
INTERMEDIATE FAVORABLE-RISK (GS 3+4=7 & PSA <20)									
MB0256-10-12	23.6	49.3	27.1	Stable	3.62 (10/12)	3+4 (03/13)	Active Surveillance	54	11.7
MB0256-03-13	27.8	44.0	28.2		5.68 (03/13)			62	12.2
MB0241-08-12	20.0	53.2	26.8	Minor Change	5.71 (07/12)	3+4 (11/12)	Active Surveillance	40	11.0
MB0241-01-13	20.6	60.0	19.4		4.36 (03/13)			51	11.3
MB0266-11-12	29.4	48.4	22.2	Significant Change	7.60 (06/12?)	3+4 (10/12)	Active Surveillance	58	11.3
MB0266-05-13	23.7	50.2	26.1		10.46 (05/13)			97	16.4
MB0211-05-12	7.0	48.2	44.8	Significant Change	6.04 (01/12)	3+4 (05/12)	Radical Prostatectomy with Bilateral Lymphadenectomy (05/12)	27	13.0
MB0211-09-12	76.4	22.1	1.5		<0.01 (09/12)			288	18.0
MB0211-01-13	27.4	49.8	22.8		<0.01 (01/13)			57	12.8
MB0235-08-12	16.7	54.0	29.3	Significant Change	5.71 (12/11)	3+4 (08/12)	Radical Prostatectomy with Bilateral Pelvic Lymphadenectomy (08/12)	24	11.3
MB0235-04-13	37.7	42.7	19.6		<0.01 (04/13)			68	11.8
MB0218-06-12	12.7	64.0	23.3	Significant Change	1.85 (06/12)	3+4 (11/11)	Cryotherapy (05/12)	32	11.2
MB0218-01-13	22.7	48.1	29.2		4.24 (01/13)			55	13.3
INTERMEDIATE UNFAVORABLE RISK (GS 4+3=7 and PSA >20)									
MB0240-08-12	5.4	47.6	47.0	Stable	<0.01 (07/12)	4+3 (10/07)	Radical Prostatectomy with Bilateral Pelvic Lymphadenectomy (07/10)	21	17.1
MB0240-05-13	18.3	42.4	39.3		<0.01 (05/13)			26	12.6
MB0258-10-12	40.2	45.5	14.3	Significant Change	7.50 (08/11)	4+3 (01/13)	Radical Prostatectomy with Bilateral Lymphadenectomy (01/13)	77	11.1
MB0258-04-13	34.0	50.7	15.3		<0.01 (03/13)			102	11.4
HIGH RISK (GS ≥8)									
MB0212-05-12	5.6	38.0	56.4	Significant Change	14.59 (05/12)	4+5 (03/12)	Bicalutamide 50 mg (05/12)-(07/12) Goserelin 10.8 mg (07/12-06/13) RT (08/13)	22	14.3
MB0212-12-12	13.8	64.7	21.5		0.47 (11/12)			85	15
MB0212-06-13	20.4	48.8	30.8		0.36 (05/13)			46	11.3
MB0261-11-12	25.7	50.3	24.0	N/A	11.15 (09/12)	4+5=9 (11/12)	Bicalutamide 50 mg (02/12-04/12)	85	13.0

Table 2: Clinical and Molecular Characteristics of Prostate Cancer Patients.
Comparison of PSA, Gleason scores and telomeric parameters of patients in different clinical classes. Telomeric analysis shows stable, minor and significant changes in telomeric profiles.

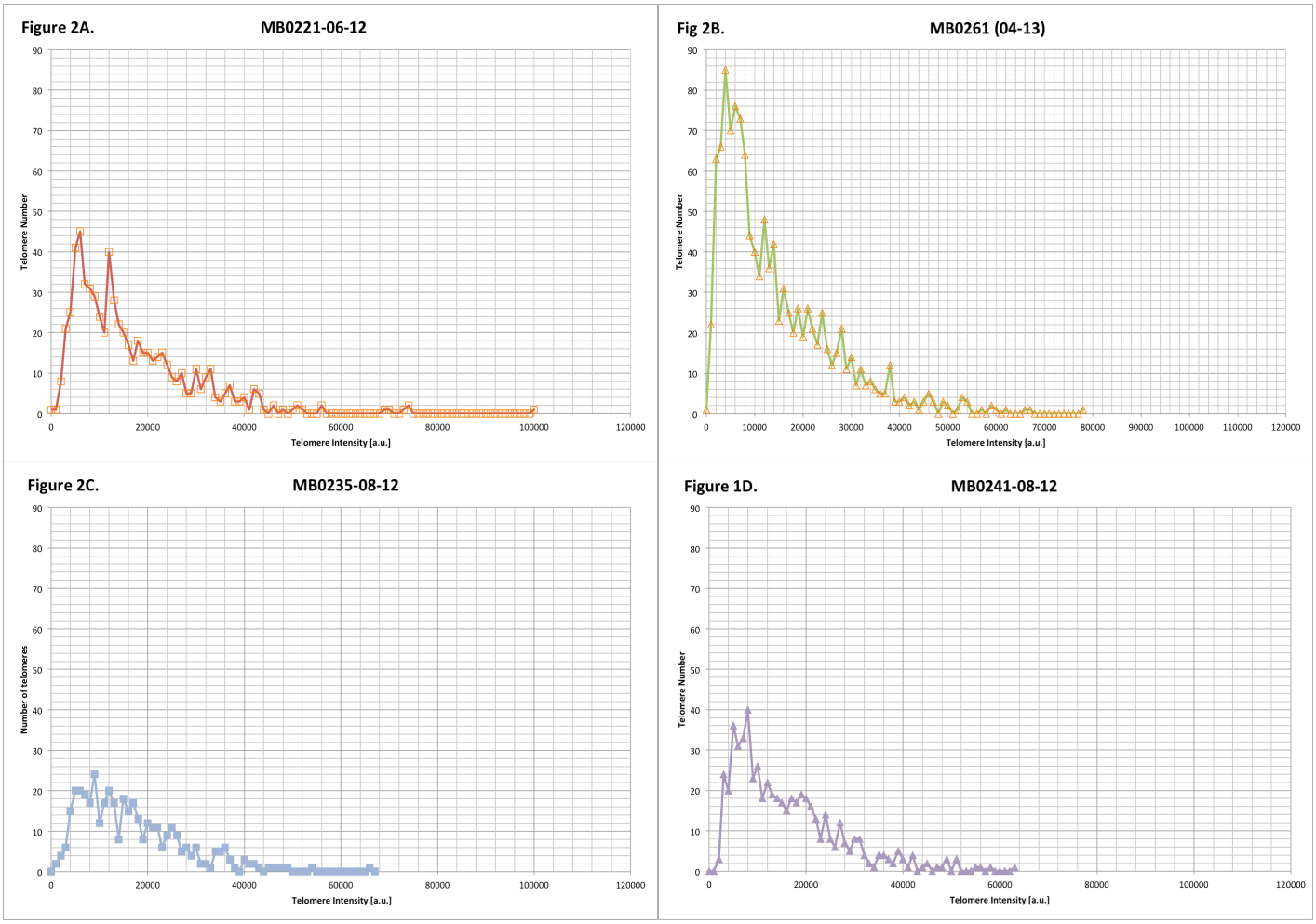

Figure 2: Teloview^{TM} Graphs of Patients with Different Clinical Profiles.
Graphs A-D are derived from Teloview^{TM} and plot telomere number against telomere intensity for patients MB0221, MB0261, MB0235, and MB0241.

A) MB0221 a low-risk patient with a clinical profile of Gleason 3+3=6 and PSA=5.13. The graph shows a wide distribution of telomere intensities and an intermediate peak telomere number (PTN).
B) MB0261 a high-risk non-metastatic patient with a clinical profile of Gleason 4+5=9. This patients graph demonstrates a high single homogeneous peak with a high number of short telomeres. A “cliff” peak can be appreciated in this patient’s graph.
C) MB0235 a favorable intermediate-risk patient with a clinical profile of Gleason 3+4=7 and PSA ≤20. The graph demonstrates three sub-populations of telomeres.
D) MB0240 an unfavorable intermediate-risk patient with a clinical profile of Gleason 4+3=7 and PSA >20. The graph demonstrates three sub-populations of telomeres.

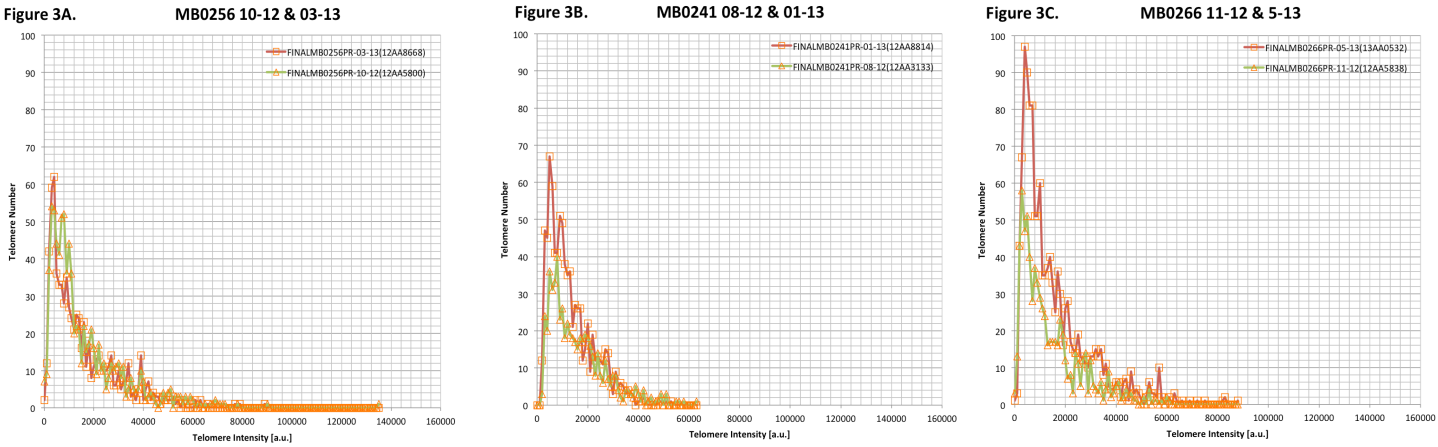

Figure 3: Progression of Telomere Profiles in Patients on Active Surveillance.
Using three favorable intermediate-risk patients all enrolled in an active surveillance program we can appreciate the varied progression of a telomere profile when medical intervention is withheld. The green curve represents the first sample examined and the red curve depicts the repeat sample examined at a later time point.

A) MB0256 shows a stable telomere profile between November 2012 and March 2013
B) MB0241 shows a minor change in the telomere profile between August 2012 and January 2013
C) MB0266 shows a substantial change in the telomere profile between November 2012 and May 2013

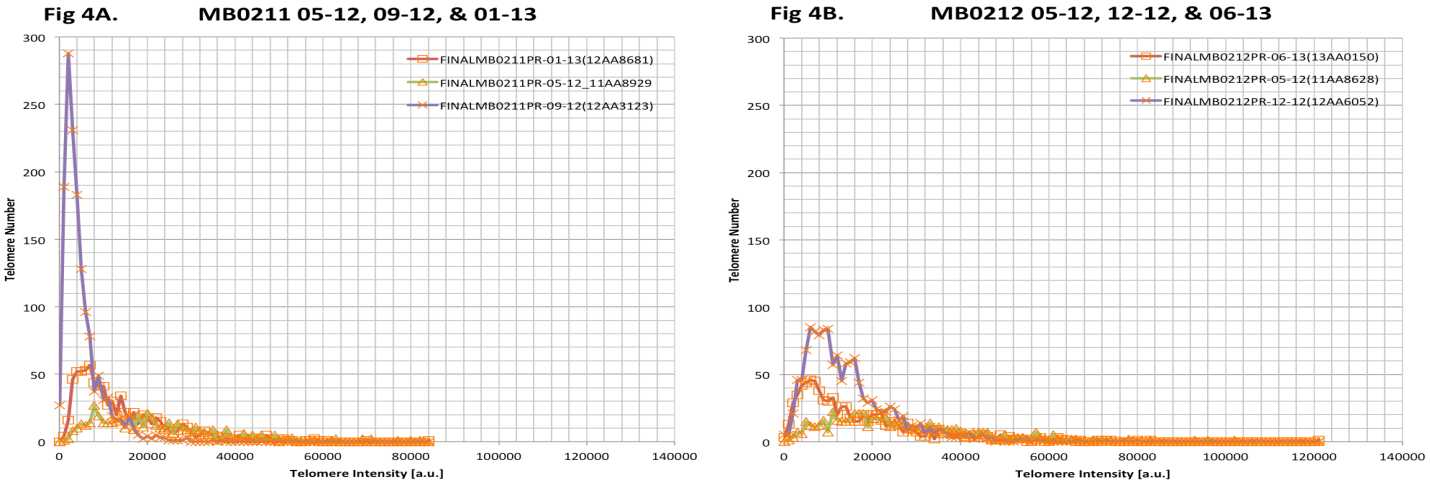

Figure 4: Progression of Telomere Profiles in Patients Undergoing Treatment.
Using two patients undergoing either medical management or surgery to control their disease, we can appreciate the change in the telomere profile during and after therapy. The green curve represents the first time point sampled, the purple curve represents the second time point sampled, and the red curve depicts the third time point sampled.

A) MB0211 shows a significant increase in his PTN following radical prostatectomy, and then a significant decrease in his PTN in the surveillance period that follows.
B) MB0212 shows a significant increase in his PTN following medical therapy with Bicalutamide and Goserelin and then a significant decrease in his PTN in the surveillance period that follows.